New Journal of Physics
The open-access journal for physics

Plasma wakefield acceleration experiments at FACET

M J Hogan[1], T O Raubenheimer[1], A Seryi[1], P Muggli[2], T Katsouleas[3], C Huang[4], W Lu[4], W An[4], K A Marsh[4], W B Mori[4], C E Clayton[4] and C Joshi[4,5]

[1] SLAC National Accelerator Laboratory, Menlo Park, CA 90309, USA
[2] University of Southern California, Los Angeles, CA 90089, USA
[3] Pratt School of Engineering, Duke University, Durham, NC 27708, USA
[4] University of California Los Angeles, Los Angeles, CA 90095, USA
E-mail: joshi@ee.ucla.edu

New Journal of Physics **12** (2010) 055030 (19pp)
Received 2 March 2010
Published 28 May 2010
Online at http://www.njp.org/
doi:10.1088/1367-2630/12/5/055030

Abstract. FACET—Facilities for Accelerator science and Experimental Test beams at SLAC—will provide high-energy-density electron and positron beams with peak currents of roughly 20 kA that will be focused down to a 10 μm $\times$ 10 μm transverse spot size at an energy of $\sim$23 GeV. With FACET, the SLAC linac will support a unique program concentrating on second-generation research in plasma wakefield acceleration. Topics include high-gradient electron acceleration with a narrow energy spread and preserved emittance, beam loading and high-gradient positron acceleration. This paper describes the FACET facility, summarizes the state of the art for plasma wakefield accelerators and discusses the plasma wakefield accelerator program to be conducted at FACET over the next five years.

[5] Author to whom any correspondence should be addressed.

Contents

1. Introduction

In the past decade, the plasma wakefield accelerator (PWFA) has arguably emerged as a promising candidate for advanced high-energy accelerators, thanks to progress on a number of fronts [1]. Experiments conducted by the SLAC/UCLA/USC E-157/162/164/167 collaborations at the Final Focus Test Beam (FFTB) facility at Stanford Linear Accelerator Center (SLAC) have shown that plasmas can accelerate and focus both high-energy electron and positron beams [2, 3]. In addition, they have demonstrated a variety of new effects, such as the collective refraction of a charged particle beam at a plasma–neutral vapor interface [4], the generation of betatron x-rays from a few keV to tens of MeV [5], and the acceleration of electrons from the plasma itself to more than 10 GeV by high-gradient wakefields [6]. Striking results have been found in experiments using a short ($\sigma_z \sim 15\,\mu$m), high-peak-current electron beam that field-ionizes a neutral lithium vapor to produce meter-scale plasmas [7]. Accelerating wakefields in excess of 50 GeV m^{-1} have been sustained in 85 cm long plasma using a 42 GeV drive electron beam [8]. This gradient is roughly 3000 times that in the SLAC linac, and the wakefield in this meter-scale plasma has accelerated some of the electrons in the back of the bunch itself to energies up to 85 GeV.

Continued progress towards developing the PWFA scheme into a practical accelerator [9] operating at the energy frontier of high-energy physics requires that issues such as energy spread, beam emittance and beam loading efficiency—for both electron and positron beams—that have hitherto not been addressed should be examined experimentally. In order to do this, appropriate high-energy beam facilities are critically important. Early PWFA experiments were carried out at the Argonne Wakefield Acceleration Facility [10] using modest energy and current electron beams. However, rapid progress occurred when increasingly high-intensity bunches from the SLAC linac became available for PWFA experiments [11] at the FFTB.

The FFTB was recently decommissioned for construction of the linear coherent light source (LCLS) and is being replaced with a new facility: Facilities for Accelerator science

Table 1. Legend of symbols used in this paper.

Physical parameter	Symbol	Physical parameter	Symbol
Speed of light in vacuum	c	Plasma density	n_{p}
Charge of an electron	e	Drive beam transverse size	σ_r
Classical electron radius	$r_e - e^2/4\pi\varepsilon_0 m_e c^2$	Drive beam bunch length	σ_z
Accelerating gradient	eE	Beam plasma frequency	$\omega_{\mathrm{pb}} = (n_{\mathrm{b}} e^2/\varepsilon_0 m_{\mathrm{e}})$
Plasma focusing gradient	$K = \omega_{\mathrm{p}}/(2\gamma)^{1/2} c$	Electron plasma frequency	$\omega_{\mathrm{p}} = (n_0 e^2/\varepsilon_0 m_{\mathrm{e}})$
Plasma wavenumber	$k_{\mathrm{p}} = \omega_{\mathrm{p}}/c$	Beta function of the beam	$\beta = \gamma\sigma_r^2/\varepsilon_{\mathrm{N}}$
Plasma wavelength	$\lambda_{\mathrm{p}} = 2\pi/k_{\mathrm{p}}$	Normalized emittance	$\varepsilon_{\mathrm{N}} = \gamma\varepsilon$
Mass of an electron	m_{e}	Spot size in x, y	σ_x, σ_y
Electrons per bunch	N	Focal length in x, y	f_x, f_y
Drive beam density	$n_{\mathrm{b}} = N/(2\pi)^{3/2}\sigma_r^2\sigma_z$	Skin depth of plasma	c/ω_{p}

and Experimental Test beams (FACET). FACET will provide high-energy, high-peak-current, low-transverse-emittance electron and positron beams and the corresponding experimental infrastructure. The primary focus of FACET will be the continued development of PWFAs, although there will be other important science areas that will benefit from the availability of FACET beams [12]. The main goals of the PWFA experiments on FACET are to demonstrate significant energy gain by electron and positron bunches in a single, high-gradient PWFA stage while preserving the beam emittance and a small momentum spread, and demonstrating a reasonable energy transfer efficiency.

2. The plasma wakefield accelerator (PWFA)

The basic concept of the PWFA involves the passage of an ultrarelativistic charged particle bunch through a stationary plasma [13]. The plasma may be formed by ionizing a gas with a laser [14] or through field ionization by the Coulomb field of the relativistic bunch itself [7]. This second method allows the production of meter-long, dense (10^{16}–10^{17} cm^{-3}) plasmas suitable for the PWFA and greatly simplifies the experimental setup. In single-bunch experiments carried out with ultrashort electron bunches, the head of the bunch creates the plasma and drives the wake [7]. The wake produces a high-gradient longitudinal field that in turn accelerates particles in the back of the bunch. The system effectively operates as a transformer, where energy from particles in the bulk of the bunch is transferred to those in the back, via the plasma wake. The physics is unchanged if there are two bunches rather than a single bunch; energy from the leading drive bunch is transferred to a trailing witness bunch.

In a PWFA operating in the so-called blowout regime, a short but high-current electron bunch, with density n_{b} larger than the plasma density n_{p} (for definitions of all the symbols used in this paper, refer to table 1), expels all the plasma electrons from a region surrounding the beam [15]. The expelled plasma electrons rush back in because of the restoring force of the relatively immobile plasma ions and thus generate a large plasma wakefield. This wakefield has a phase velocity equal to the beam velocity ($\cong c$ for ultrarelativistic beams). Since the electrons in the bunch are ultrarelativistic, there is no relative phase slippage between the electrons and the wake over meter-scale plasmas. The FFTB experiments used this important fact not only to excite the wake, but also to probe the wakefield by monitoring the energy change—both energy loss and gain—of electrons within a single drive bunch. This case is schematically depicted in

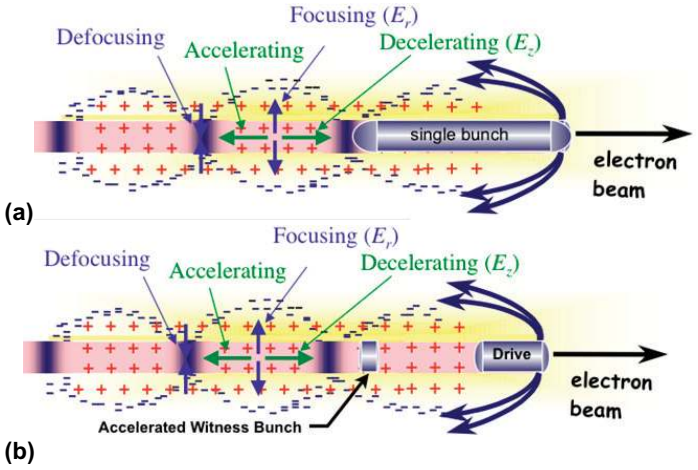

Figure 1. Physical mechanism of the PWFA for previous single-bunch experiments in the FFTB (a) and the two-bunch case proposed for FACET (b). The multiple wavelengths (buckets) of the wakefield are the result of plasma electron overshooting as they cross the ion column axis.

figure 1(a). Ideally, one would instead place a separate, short 'witness' bunch at the appropriate phase behind the drive bunch and containing a sufficient charge to be efficiently accelerated, as schematically shown in figure 1(b). Appropriate techniques to craft two bunches spaced in time by roughly one plasma period are an integral component of the second-generation plasma experiments proposed for FACET.

According to linear plasma theory [16, 17], for a single bunch with a normalized transverse beam size $k_p\sigma_r \ll 1$, the accelerating field is maximized for $k_p\sigma_z \approx \sqrt{2}$, i.e. when the plasma electrons rush back on the axis immediately behind the bunch. In this regime, linear theory predicts a maximum accelerating field given by [18]

$$eE_{\text{linear}} \cong 100\,\text{GeV/m}\left(\frac{N}{2\times10^{10}}\right)\left(\frac{20}{\sigma_z(\mu\text{m})}\right)^2 \ln\sqrt{\frac{2.5\times10^{17}(\text{cm}^{-3})}{n_p}\frac{10(\mu\text{m})}{\sigma_r}}, \quad (1)$$

where N is the number of particles in the electron bunch, σ_z is bunch length, n is plasma density and σ_r is spot size. Linear theory is valid when the normalized charge per unit length of the beam, $\Lambda \equiv \frac{n_b}{n_0}(k_p\sigma_r)^2 \cong 2.5(\frac{N}{2\times10^{10}})(\frac{20}{\sigma_z(\mu\text{m})})$, is less than 1. For high Λ the nonlinear equivalent of equation (1) [18, 19] should be used.

Equation (1) indicates that generating large-amplitude wakefields requires short, high-density electron bunches. For the same total charge in the drive beam, if the wake is excited in the blowout regime by focusing the beam tighter ($n_b > n_p$ and $k_p\sigma_r \ll 1$ but $\Lambda > 1$) [17]–[20], the wake excitation is highly nonlinear (spiky, see figure 2(a)) and can reach a peak value $(eE)_{\text{peak}}$ of up to four times$(eE)_{\text{linear}}$. For the portion of the wake that can be used to effectively accelerate particles (labeled as usable field in figure 2(a)), the amplitude is roughly 0.5 of the peak. Particle-in-cell (PIC) code simulations and the nonlinear theory of Lu *et al* (if the bunch length is matched nonlinearly) of wakes, however, show that the $1/\sigma_z^2$ scaling of usable electric field still holds even in the nonlinear regime, as indicated in figure 2(b). Further optimization is possible in the nonlinear regime by optimizing the spot size as well as the plasma density [21].

Experiments in the FFTB addressed key questions of the magnitude and sustainable length for the accelerating field of a beam-driven wake produced in a plasma [22]. These experiments

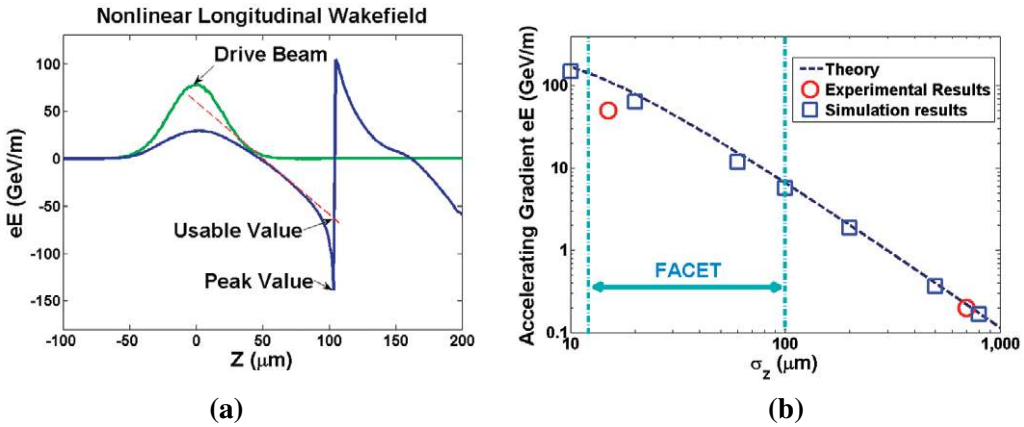

Figure 2. (a) Nonlinear longitudinal wakefield excited by the drive beam in a plasma. (b) Peak accelerating field versus drive electron bunch length for $N = 2 \times 10^{10}$ electrons for a fixed beam spot size of $5\,\mu$m. The density is varied such that the normalized bunch length is kept fixed at $k_p\sigma_z = \sqrt{2}$. As the bunch length is shortened, there is a transition from the linear to the nonlinear regime. The dashed line is the prediction from linear theory for narrow bunches (equation (1)). The squares are the results obtained from QuickPIC simulations. The circles are experimental data points. Note that in the experiments the bunch length is not exactly matched to $k_p\sigma_z = \sqrt{2}$. When the exact experimental parameters are simulated, the gradients are in agreement, e.g. see [8].

have demonstrated, as shown in figure 2(b), the dramatic increase in accelerating gradients predicted by equation (1) as the bunch length is reduced. The ion column generated by the head of the bunch provided a very large focusing gradient ($\approx 3\,\mathrm{MT\,m^{-1}}$ or $n_p = 10^{17}\,\mathrm{cm^{-3}}$), which maintained the beam density by guiding the beam [23] and allowed the beam to drive the wake over an extended distance. The combination of large focusing and accelerating gradients led to large energy gains (shown in figure 3) using ultrashort, 42 GeV electron bunches, where some of the electrons doubled in energy [8] in just 85 cm of plasma with a density of $2.7 \times 10^{17}\,\mathrm{cm^{-3}}$.

Current and proposed experiments operate in a regime where linear plasma theory is not valid. To help interpret the experimental data and design new experiments, two numerical codes are used, OSIRIS [24] and QuickPIC [25]. OSIRIS is a three-dimensional (3D), fully electromagnetic, relativistic, parallelized PIC code that has been benchmarked against other codes and model problems that can be solved analytically. QuickPIC is a 3D, PIC code that uses a quasi-static approximation to decrease the computing time. OSIRIS and QuickPIC include the effects of field ionization and electron beam energy loss due to radiation from oscillations in the ion column. OSIRIS and QuickPIC are now the standard tools for simulating beam–plasma interactions in experiments proposed at FACET. These codes have successfully described many of the observed phenomena in a quantitative manner [4, 6, 7, 24] and are being used to design the future plasma wakefield accelerator linear collider (PWFA-LC).

3. PWFA experiments at FACET

FACET will demonstrate the high-gradient acceleration of a witness bunch with low energy spread and high beam loading (energy extraction efficiency). Furthermore, the emittance

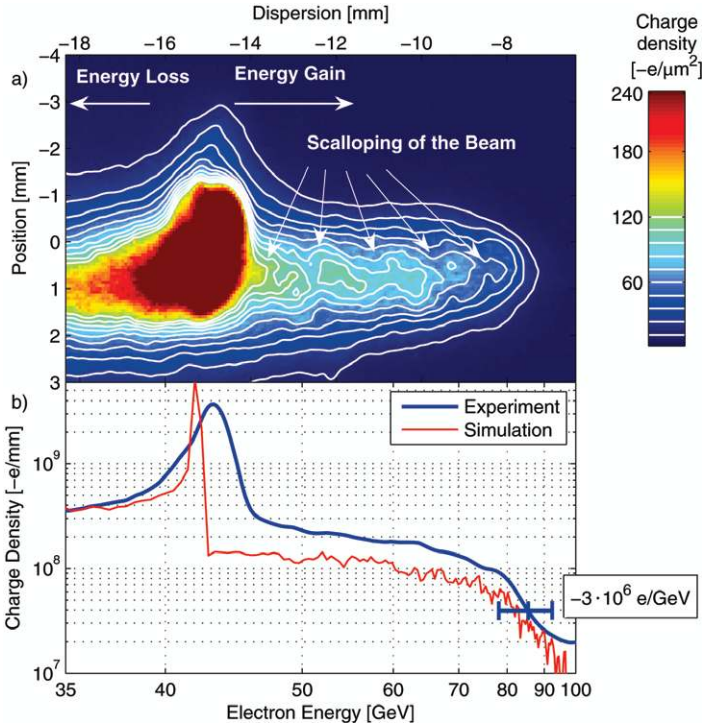

Figure 3. (a) Energy spectrum of electrons in the 30–100 GeV range. The head of the pulse, which is unaffected by the plasma, appears at −15 mm, equivalent to 43 GeV. The core of the pulse, which has lost energy driving the plasma wake, is dispersed partly out of the left field of view of the camera. Particles at the back of the bunch, which have reached energies up to 85 GeV, are visible to the right. The pulse envelope exits the plasma with an energy-dependent phase advance, which is consistent with the observed scalloping of the dispersed beam. (b) Projection of the image in (a), shown in blue. The simulated energy spectrum is shown in red. The difference between the measured and the simulated spectra near 42 GeV is due to an initial correlated energy spread of 1.5 GeV not included in the simulations. (Adapted from [8].)

dilution mechanisms for an electron drive and electron witness bunch will be measured. Next, FACET will be used to characterize high-gradient positron acceleration using first a positron drive beam and then an electron drive beam. After understanding the options, a positron acceleration scheme will be selected and demonstrated at FACET with high gradient, low energy spread and high beam loading.

3.1. The FACET facility

The main parameters of the electron beam from FACET are summarized in table 2. FACET beams have energy densities exceeding 1 MJ cm^{-2} and intensities exceeding 1×10^{20} W cm^{-2} at a repetition rate of 10 Hz. Thus, FACET beams are excellent sources of energy to drive wakes in plasmas over long distances and to produce energy gain of the order of 25 GeV. The facility will be located upstream of the LCLS injector, as illustrated in figure 4. FACET will use the first

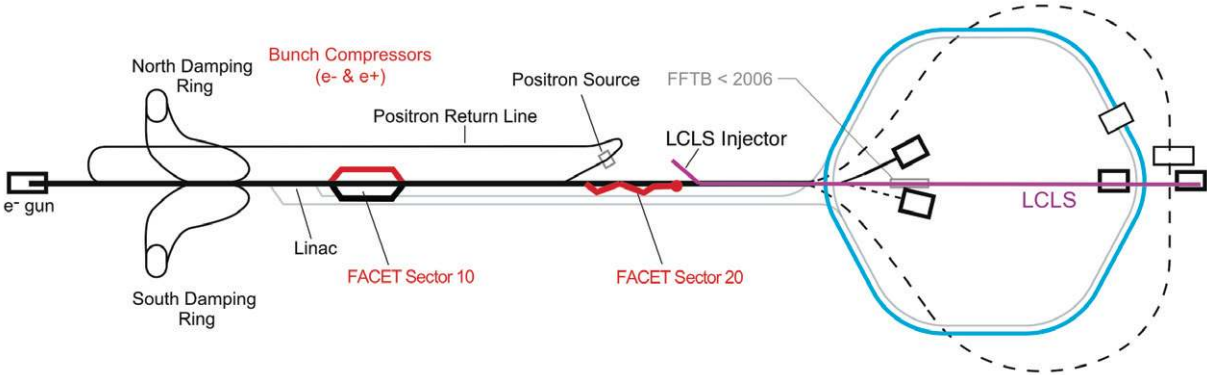

Figure 4. Schematic of the SLAC site with proposed FACET modifications to the linac systems marked in red. The positron bunch compressor is at Sector 10 and the experimental area is at Sector 20 along the linac. A shielding wall at the end of Sector 20 will allow access to the upstream portion of the linac during LCLS operations.

Table 2. FACET beam parameters.

Energy	23 GeV with full compression and maximum peak current
Charge per pulse	3 nC per pulse with full compression
Pulse length at the focal point or interaction point IP (σ_z)	25 μm with 4% full-width (fw) momentum spread with full compression and 40 μm with 1.5% fw momentum spread with partial compression
Transverse spot size at IP ($\sigma_{x,y}$)	$<$10 μm nominal
Momentum spread	4% full-width with full compression (3% full-width at half-maximum (FWHM)) $<$0.5% full width without compression
Momentum dispersion at IP (η and η')	0
Drift space available for experimental apparatus	2 m from the last quadrupole to the focal point; approximately 23 m from the focal point to the beam dump
Transverse space available for experimental apparatus	3 m (width)$\times$3 m (height)

2 km of the SLAC linac to produce approximately 23 GeV electron and positron beams with small emittances.

A final focus system and an experimental area have been designed to fit in the existing linac tunnel in Sector 20. The Sector 20 beam line will consist of a chicane, which has four dipole magnets to compress the beam longitudinally followed by an arrangement of quadrupole magnets to focus the beam to an interaction point near the middle of the sector. Tracking programs that include second-order effects have been used to verify the FACET beam parameters summarized in table 2. This new—Sector 20—beam line will start downstream of the positron production extraction point (where electrons are directed to the positron production target) and extend to a new beam dump near the end of Sector 20, a few meters upstream of

the point where the LCLS injector line enters the linac tunnel. Comparable beam parameters for positron beams will be achieved with the addition of an upstream positron bunch compressor in Sector 10. At this location an electron bunch compressor or a magnetic chicane already exists.

3.2. Producing high-intensity drive bunches

The dramatic increase in the maximum particle energy produced by PWFA is a direct result of the advent of high-intensity drive bunches at SLAC. There are two factors involved in achieving the high intensities needed for exciting large-amplitude wakes—a high peak current and a small transverse size.

The high peak current will be achieved in FACET by making use of a threefold compression process similar to that used for the FFTB experiments [26]. Longitudinal compression is accomplished by manipulating the longitudinal phase space of electron bunches, which has a constant area after the exit from the north damping ring. The nominal three-stage compression process is described below and illustrated in figure 5.

The electron bunch is produced by an electron gun and accelerated to an energy of 1.19 GeV. Its normalized emittances are lowered to $\varepsilon_{Nx} = 50$ and $\varepsilon_{Ny} = 5$ mm mrad in the north damping ring (see figure 4). When exiting the damping ring, the bunch is ∼5.5 mm long and has a very small uncorrelated energy spread of ∼0.07% (figure 5(a)). The long bunch travels in an rf cavity at the zero crossing of the rf accelerating wave, which leaves its average energy unchanged. However, the cavity electric field imparts a correlated energy spread of ∼1% to the bunch (figure 5(b)). The bunch then travels through the ring to the linac beam line in which the momentum compression factor (R_{56}) compresses the bunch to 1.5 mm (figure 5(c)). In the first kilometer of the linac, the bunch is accelerated to 9 GeV while riding off the accelerated rf wake crest by about 20° of longitudinal phase. As a result, the bunch reaches the magnetic compressor chicane located in Sector 10 (see figure 4) with a new correlated energy spread of ∼1.6% (figure 5(d)). The chicane compresses the bunch to ∼60 μm (figure 5(e)). Along the second kilometer of the linac, the bunch is accelerated to its final energy of 23 GeV. During this process the bunch loses energy to longitudinal wakefields, and acquires a third correlated energy spread of 1.3% (figure 5(f)). The bunch experiences its final compression in the FACET experimental hall and reaches a minimum length of 14 μm and a peak current in excess of 20 kA (figure 5(g)).

3.3. Plasma production by field ionization

In addition to high-intensity beams, producing a large energy gain requires uniform, high-density meter-scale plasmas. When the current density of the electron bunch is high enough, the Coulomb field of the relativistic electron bunch can create a plasma in a tube of vapor through field or tunnel ionization. The ionization is accomplished by leading particles of the drive bunch, so the majority of that bunch and any trailing bunches encounter a fully ionized plasma. Field ionization has allowed for the production of long, uniform, high-density alkali metal (Li, Rb or Cs) plasmas with no timing or alignment issues [7]. This technique may allow the production of uniform high-density plasmas that are 10 m or more in length, which are needed for future plasma-based colliders.

Alkali vapor is created in a heat pipe oven [27] where neutral vapor density and length are controlled by the pressure of a buffer gas (He, Ar, etc) and heating power to the oven.

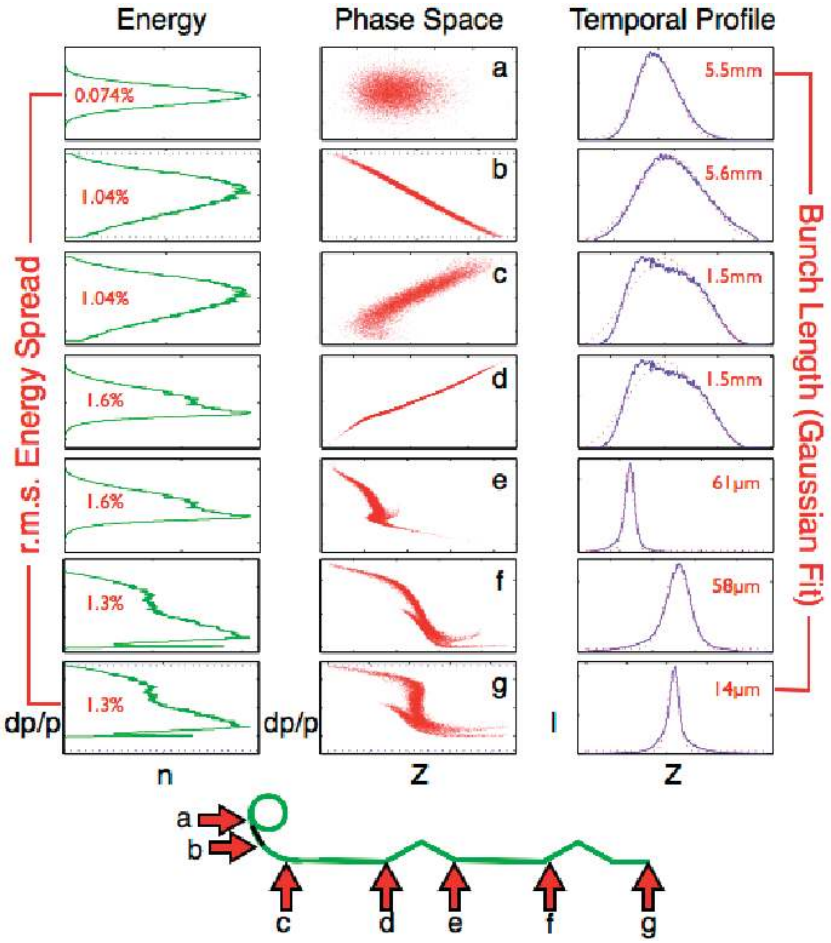

Figure 5. Evolution of longitudinal phase space of the FACET beam as seen in a 2D particle tracking simulation, illustrating the three-stage compression process that yields a beam with a 14 μm rms bunch length and a 22 kA peak current. The middle column (a)–(g) shows the bunch phase space, i.e. the relative longitudinal momentum of particles ($\Delta p_z/p_z$) versus position along the bunch at the locations along the linac indicated by the red arrows on the linac schematic, also labeled (a)–(g). The left-hand-side column shows the corresponding relative momentum spectra (projection of phase space along z). The right-hand-side column shows the corresponding bunch current profile (projection of phase space along $\Delta p_z/p_z$).

The buffer gas confines the hot alkali vapor at both ends. Lithium, for instance, has a relatively low ionization potential for the first electron (5.4 eV), allowing complete ionization of lithium vapor to generate densities of up to 4×10^{17} cm^{-3} over a broad range of beam parameters. The larger ionization potential of the second electron of the Li atom (75.6 eV) ensures that the plasma density does not evolve significantly along the bunch due to secondary ionization. The plasma density is then equal to the lithium vapor density.

An important issue in FACET experiments might be beam head erosion resulting from nonzero beam emittance [28] in the tunnel-ionized plasma. This effect was identified as the

limiting factor for maximum energy gain in the FFTB experiments. As we shall see below, the generation of two bunches, needed to perform a drive beam/witness beam experiment at FACET, will reduce the peak current in the drive beam compared to the E167 experiment [8]. This may delay the onset of field ionization and exacerbate beam head erosion in a lithium plasma. To mitigate this effect, we are planning on using lower-ionization-potential alkali atoms such as rubidium or cesium, and are also exploring the use of pre-ionized laser-produced plasma columns.

3.4. Two-bunch experiments

In PWFA experiments at the FFTB, the large-amplitude wakefield was both created and sampled by a single bunch, resulting in a continuous energy spread in particles emerging from the plasma, as shown in figure 3. A future PWFA-LC must accelerate a separate witness bunch with a finite energy spread. Demonstrating this capability requires the production of two distinct bunches separated by a fraction of a plasma wavelength ($\sim$100 μm for plasma and beam parameters considered at FACET). Until recently, there has been no technique capable of producing the short, high-peak-current drive bunches required to produce a large wake, while simultaneously creating a following trailing bunch to sample and load the accelerating portion of the wake.

FACET will use a mask installed in the final bunch compressor chicane to create the two bunches needed for these experiments. The mask concept has the ability to make several bunches from a single initial bunch, and has been recently demonstrated experimentally [29].

The concept is as follows. In the middle of the final chicane, the electron (or positron bunch) is dispersed according to its energy. Since for the compression process the bunch must have a correlated energy spread (see figure 5(f)), there is a correlation between position along the dispersion plane and time along the bunch. A solid mask a fraction of a radiation length thick (made of tantalum or some other high-Z material) is placed at a location where the beam size (along the dispersion plane) is dominated by its energy spread. Particles hitting the solid parts of the mask are scattered and, as a result, the emittance of time slices of the bunch is greatly increased. Upon leaving the chicane, the dispersion is brought back to zero, and the mask spatial pattern is imprinted onto the bunch current profile. Longitudinal time slices of the beam with their emittance spoiled by the mask are progressively lost along the beam line. At the same time, the bunch is not fully compressed to preserve the time structure of the bunch.

The masking process is modeled in six dimensions (x, x', y, y', t, p) with a combination of tracking codes linked together by MATLAB. ELEGANT [30] is used to track the beam from the exit of the north damping ring to the middle of the linac bunch compressor chicane in Sector 10. The particles are then converted into an appropriate input for EGS4 [31] via the program SHOWER [32]. The mask and the vacuum region around it are simulated with EGS4. The EGS4 output is then converted and loaded back into ELEGANT for tracking to the exit of the chicane and on to the FACET focal point.

Figure 6 shows an example of the bunch train structure that can be produced using the procedure mentioned above. In this case, the mask includes two solid parts that spoil the emittance of low- and high-energy bunch particles. These are used to get rid of the long temporal tail that results from the nonlinearity in the compression process and is visible in figure 5(g). At the same time, a solid blade is also placed near the middle of the bunch energy spectrum in order to produce separate drive and witness bunches with appropriate parameters for the PWFA experiments. Figure 6(a) shows an example of the phase space (particle density in $\Delta p_z/p_z$ versus

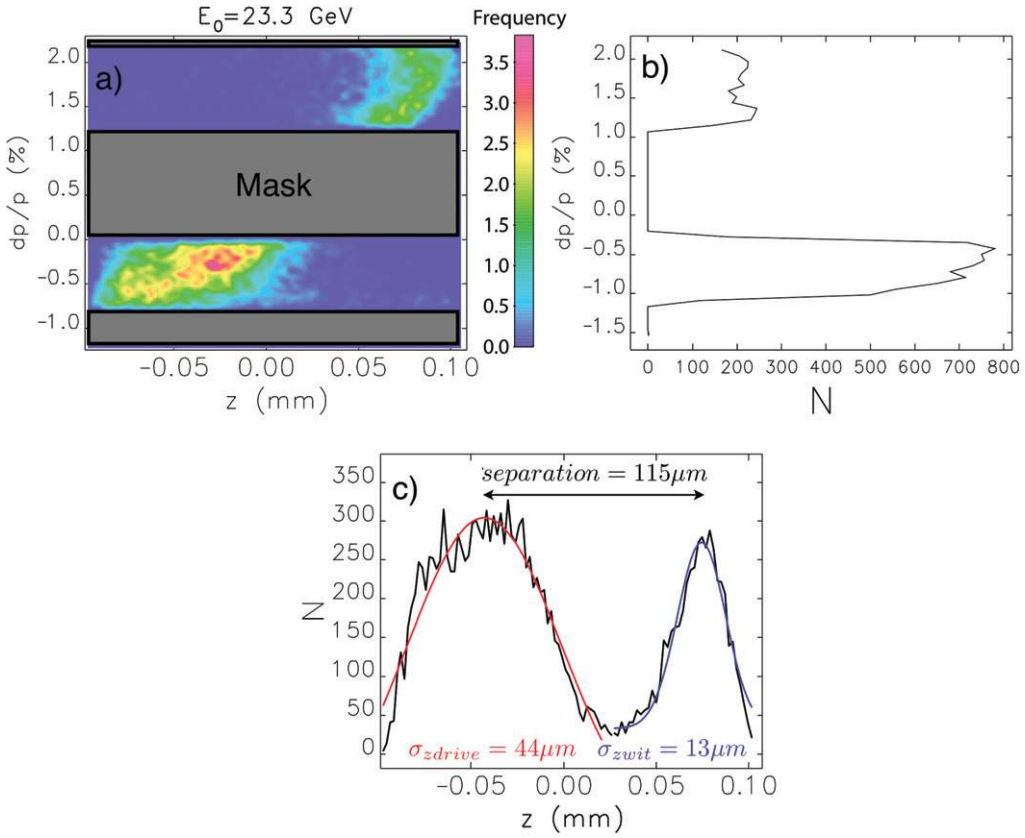

Figure 6. (a) An example of the simulated longitudinal phase space of drive and witness bunches at the FACET focal point. The simulated bunches were created for FACET PWFA experiments using a mask technique. Panel (b) shows the energy spectrum of the bunches after the mask, and panel (c) shows their charge or current profile. The mask blades are also schematically represented in panel (a).

z space) of the beam after final compression. Here one can clearly see that particles scattered by the blade are now missing. The projection of the phase space giving the bunch energy spectrum is shown in figure 6(b). Similarly, a projection of figure 6(a) to give current versus position (z) is shown in figure 6(c). Both show a clear gap, and the consequent two-beam (drive–witness) structure that is produced by the mask. In this example the two bunches contain 6.7×10^9 (drive) and 3.3×10^9 (witness) electrons (total charge $\sim$1.6 nC). The drive bunch has a length of 18 μm and the witness 25 μm. The separation between the two bunches is 115 μm.

3.5. High-gradient acceleration experiments

Accelerating a witness bunch with a narrow energy spread but with a high efficiency to obtain a significant ($\sim$25 GeV) energy gain is the main goal of the PWFA program on FACET. Extensive series of simulations in which wakefields are excited in both self-ionized and pre-ionized plasmas have been carried out. We describe one example in some detail below.

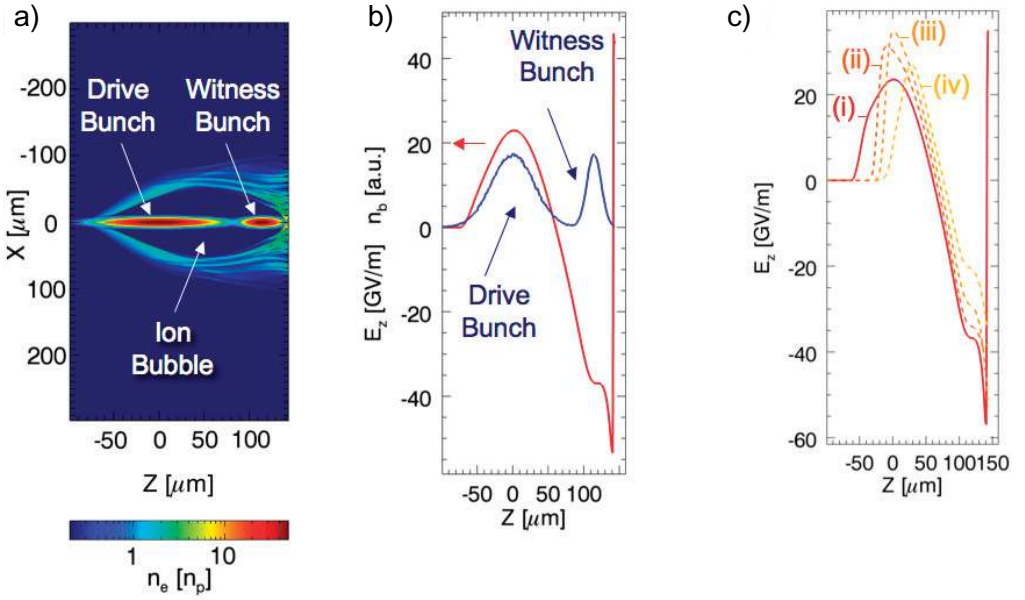

Figure 7. QuickPIC simulation results showing a PWFA utilizing a drive/witness bunch configuration produced using a mask in the dispersion plane. Panel (a) shows the plasma and beam densities at the entrance of the plasma. Panel (b) shows the positions of the two bunches relative to the longitudinal wakefield on the axis. Panel (c) shows the evolution of the wakefield at (i) $z = 0$, (ii) 28, (iii) 55 and (iv) 83 cm.

The parameters of these QuickPic simulations were as follows: the drive electron beam had a σ_z of 30 μm and contained 3×10^{10} electrons. The trailing beam had a σ_z of 10 μm and contained 1×10^{10} electrons. The separation between the drive and the witness beams was 115 μm. Both beams with an initial energy of 25 GeV were focused to a spot size σ_r of $\sim$3.28 μm in an $\sim 1 \times 10^{17}$ cm^{-3} lithium vapor. The initial normalized beam emittance was 100 mm mrad. The simulation box moving at the speed of light was 600 μm $\times$ 600 μm $\times$ 313 μm and contained $512 \times 512 \times 256$ cells. Thus in this simulation, $k_p\sigma_r = 0.2$, $k_p\sigma_z = 0.6$ and $n_b/n_p = 60$, which clearly places the experiment in the blowout regime.

Figure 7(a) shows the beam and plasma density as beams enter the plasma. One can clearly see that the drive beam has completely blown out all the plasma electrons and has created an ion bubble. Figure 7(b) shows the relative position of the two beams within the longitudinal field E_z of the wake. The peak decelerating field is close to the peak of the drive bunch ($z = 0$), as expected. The accelerating field is highly nonlinear with the characteristic narrow spike, with a peak gradient of 53 GV m^{-1}. However, beam loading leads to damping of this spike. The transformer ratio R (the peak accelerating field divided by the peak decelerating field) as seen by the peak of the trailing bunch is 1.6. Figure 7(c) shows the evolution of the longitudinal field at four positions along the plasma. As the drive bunch propagates through the plasma, its front slices continue to expand away due to the finite (100 mm mrad) emittance of the particles. This continuous beam head erosion pushes the position of the maximum decelerating field backward, while its magnitude at first increases from 23 GV m^{-1} at $z = 0$ to 35 GV m^{-1} at $z = 55$ cm. The transformer ratio therefore falls from an initial value of 1.6 to 0.8 at $z = 55$ cm. Thereafter, as the

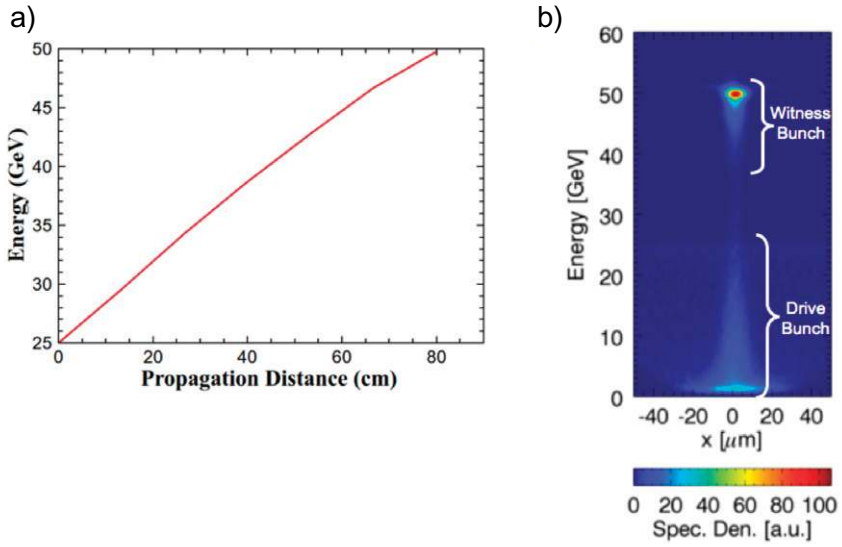

Figure 8. (a) Most probable energy of witness bunch particles as a function of propagation distance in plasma. (b) Energy spectrum of the drive and witness bunch after 85 cm of plasma.

drive bunch particles lose a significant fraction of their energy and actually begin to slow down, the position of the peak decelerating field rapidly moves back (in the speed of light frame). At the same time its magnitude drops. However, the position of the peak accelerating field (the spike in figure 7(c)), and more importantly the plateau in the acceleration field where most of the witness bunch particles reside, does not change in this frame, and the witness bunch moves with the wakefield without dephasing.

3.6. Efficiency

Figure 8(a) shows energy gain (defined as the most probable energy of the witness bunch particles) as a function of propagation distance for the simulations of figure 7. The energy gain is almost linear up to a distance of ≈ 65 cm. At a distance of 80 cm, the initially 25 GeV witness bunch has doubled in energy with an $\approx$3% energy spread, as seen in figure 8(b). While the witness bunch is monoenergetic, much of the drive bunch has lost nearly all its energy. We have estimated various efficiencies in the simulations. The energy transfer efficiency from the wake to the witness bunch is almost 56%. The efficiency from the drive to the witness bunch is greater than 30%.

The overall drive to witness bunch transfer energy efficiency can be improved by using bunches with longitudinal current profiles tailored such that all longitudinal slices of the drive bunch lose energy at the same rate (except for the very first and the last ones). This is accomplished by ramping up the current along the bunch. The optimum longitudinal current shape is trapezoidal [33] with a long rise time and a sharp fall time. In that case, the peak decelerating wakefield remains constant along the drive bunch, while the peak accelerating field left behind the bunch keeps increasing with the bunch length. The transformer ratio then scales as π times the number of plasma wavelengths covered by the bunch, and can be much larger than two. More sophisticated bunch profiles can lead to even larger enhancements of R. After first

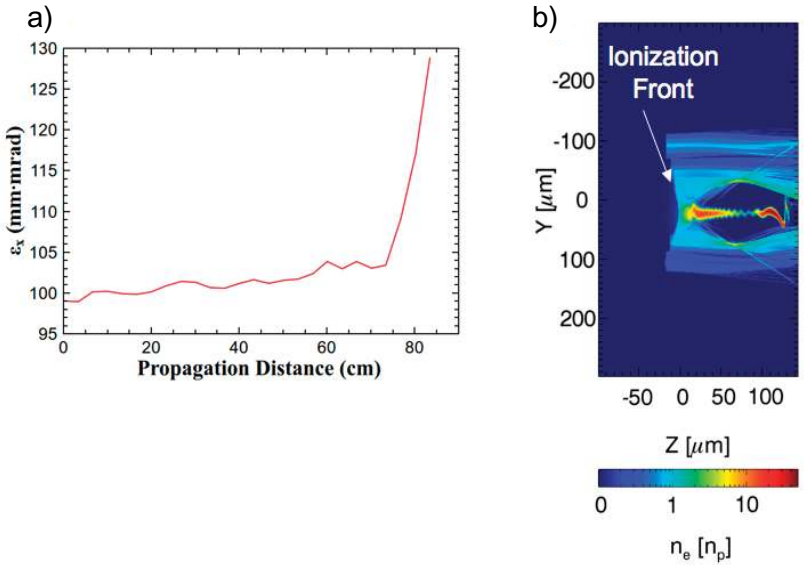

Figure 9. (a) Growth of normalized witness bunch emittance as a function of propagation distance in plasma. (b) Plasma and beam densities at the exit of the plasma ($z = -83$ cm). The ionization front location has receded close to the peak of the drive bunch at $z \approx 0$ mm (in this frame) when compared to figure 7(a), where it is at $z \approx -100$ mm. The ionization occurs over a large transverse dimension because the plasma electron sheath is less well defined and therefore provides less shielding for the electric field of the beam.

experiments with symmetric drive and witness bunches [9], FACET experiments will investigate ways of obtaining higher transformer ratios by manipulating the phase space of the bunch along the three compression stages of the linac. The compromise between optimum efficiency and beam quality will be studied and characterized.

3.7. Emittance preservation

In the blowout regime of the PWFA, all the plasma electrons are expelled from the bunch volume. As a result, the focusing force of the pure ion column is linear with radius and constant along the bunch. This has the beneficial effect of preserving the emittance of the beam that is being accelerated, provided the ions remain stationary. Figure 9(a) shows the evolution of witness bunch emittance as a function of distance for the same simulation as that of figure 7. In this case, the witness bunch is nearly matched to the plasma, and gains energy with less than 5% emittance growth up to a distance of 70 cm. Recall that at this point the drive bunch particles have significantly depleted in energy. The head to tail oscillation of the drive bunch helps to seed the hosing instability of the witness bunch, as seen in figure 9(b). The rapid blowup of the emittance of the witness bunch between 70 and 83 cm is the result of the explosive growth of the hosing instability [43]. This is clearly to be avoided in future collider applications. Note that no sign of hosing was observed in previous experiments [8, 22] when care was taken to ensure a bunch without an off-axis tail.

For the drive and witness beam parameters envisioned in the future PWFA-LC [9] the bunch density may exceed 10^{20} cm^{-3}. At such high densities the assumption that plasma ions

remain at rest for at least a plasma period breaks down as n_b/n_p approaches $m_{ion}/m_{electron}$. In this case, the drive and/or the witness bunch will impart such a large transverse momentum to the plasma ions that they will be focused onto the axis within one plasma wake period. The focusing of plasma ions will create nonlinear focusing forces that will vary along the bunch, and will result in significant emittance growth of the accelerated bunch [34].

A number of methods have been proposed to try to mitigate the effect of plasma ion motion on beam quality [35]. These include using atoms heavier than lithium for the plasma, such as Rb and Cs, using an input beam with phase space correlation to compensate for the nonlinearity of the focusing force, or using a plasma with a radial density gradient similar to that used to guide laser pulses. Alternatively, one could employ an adiabatic matching section consisting of a plasma that has ion mass decreasing along the beam path until it reaches the low ion mass of the accelerating section [36]. However, a solution has yet to be demonstrated. It is therefore important to find ways of minimizing the effect of ion motion both with numerical simulations and in experiments. The effect of plasma ion motion could be observed by measuring betatron oscillations while varying the n_b/n_p ratio or in a plasma lens experiment where the beam charge and transverse size could be varied from $n_b > n_p$ to $n_b \gg n_p$. These types of experiments are ideally performed with beams that will be available at FACET that can be focused to small transverse sizes, combined with very high peak currents, to reach densities much larger than the plasma density.

3.8. Positron acceleration

Wakes produced by a positron drive beam and subsequent acceleration of positrons are not as well studied and understood as the acceleration of electrons at the present time. All earlier experiments were carried out with longer, approximately 4 ps FWHM, positron bunches propagating through relatively low-density laser pre-ionized plasmas [37, 38]. As a result, the accelerating and focusing gradients were modest. For instance, the measured acceleration gradients were comparable to or larger than those achieved using conventional rf structures, of the order of $56\,\mathrm{MV\,m^{-1}}$ [37]. Measurements also showed halo formation and emittance growth [39] of the positron beam due to the nonlinear focusing forces acting on different longitudinal slices of the beam.

A proposed concept for a future plasma-based collider [9] uses an electron drive beam to generate the accelerating field for positrons, but other concepts, such as the single- and multi-stage afterburners, employ a positron drive beam [40]–[43]. Initial studies of positron acceleration at FACET will have the goals of understanding the underlying physics of positron/plasma interaction and establishing an appropriate drive beam configuration. It will be necessary to operate in a regime where nonlinear and relativistic plasma effects are important to achieve good efficiency. In this regime, positron and electron beams are fundamentally different, because plasma electrons are repelled by an electron beam but attracted by a positron beam. In fact, the positron beam can draw plasma electrons in from various distances within a volume proportional to the cubic skin depth of the plasma, and create on-axis plasma electron densities many times the initial neutral density. The influx of plasma electrons within the beam volume can give rise to fields that are both nonlinear and more dynamic than with an electron drive beam. Nevertheless, there are scenarios where a positron-beam-driven PWFA can be operated successfully.

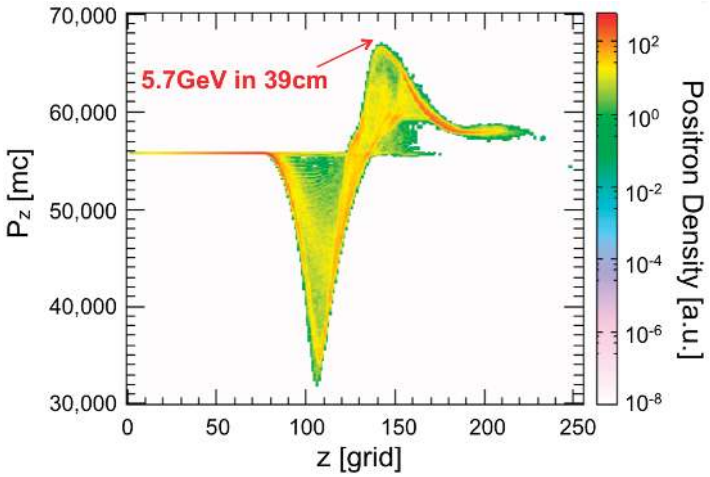

Figure 10. Simulated longitudinal phase space of a compressed positron beam after propagation through 39 cm of field-ionized plasma showing a maximum energy gain of 5.7 GeV.

We carried out numerical simulations of wake excitation and acceleration/deceleration of particles in a single positron bunch propagating through a plasma. The beam parameters of the positron beam were as follows: $N = 2 \times 10^{10}$, $\sigma_z = 15\,\mu$m, $\sigma_r = 10\,\mu$m and $\gamma_{\text{initial}} \sim 56\,000$. The beam produces plasma of density $2 \times 10^{17}\,\text{cm}^{-3}$ by field ionization. Because of the highly nonlinear nature of the focusing fields, different longitudinal slices of the beam evolve differently, producing a halo of charge around a central core. The beam erosion and hosing effects [43] are more severe when compared to a similar electron drive-beam case and limit the acceleration length. The phase space of the beam, P_z versus z, is shown in figure 10 after the beam has propagated ~0.4 m. The maximum positron energy gain is ~5.7 GeV, which implies an average peak accelerating gradient of $>14\,\text{GeV m}^{-1}$. This is orders of magnitude greater than the $56\,\text{MeV m}^{-1}$, measured with 4 ps long positron pulses [36].

First positron acceleration experiments at FACET will employ such a single compressed positron drive bunch. As with the FFTB experiments, the single bunch will sample all phases of the wakefield giving a complete picture of both the accelerating and decelerating fields involved, as shown in figure 10. Subsequent experiments will study two-bunch positron acceleration using the mask technique to demonstrate the acceleration of positrons with high gradient, good efficiency and low energy spread.

3.9. Positron acceleration in electron-driven wakes

An alternative approach for accelerating positrons is to use fields generated by an electron drive bunch. This approach offers the advantage of not requiring the large facilities necessary to create positron drive beams with megawatts of average power.

Testing this idea experimentally involves merging independent bunches of positrons and electrons produced and accelerated in the SLAC main linac. At the plasma entrance, the merged beams need to be on the same transverse orbit, with the positron bunch trailing the electron bunch by roughly one plasma wavelength (~100 μm). Initial experiments at FACET will use a simpler approach for generating positrons *in situ* within an electron-beam-driven plasma wake.

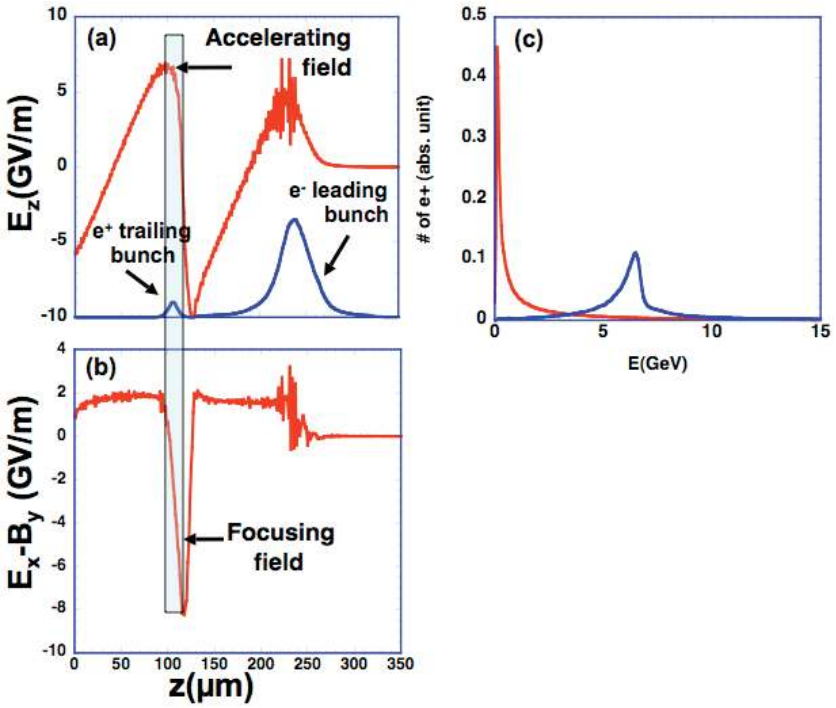

Figure 11. 3D OSIRIS simulation results showing an electron-beam-driven plasma wakefield at a distance of 9.5 cm into the plasma [44]: (a) longitudinal wakefield (E_z) lineout propagating along the z-axis; (b) transverse wakefield ($E_x - B_y$) lineout along z at $x = 4.6\,\mu$m and (c) energy spectra of the positron beam load after $s = 0.02$ cm (red line) and $s = 1$ m of plasma (blue line). The bunches shown in (a) propagate to the right. The green rectangle overlaying (a) and (b) indicates the location where the wakefields are both focusing and accelerating for positrons and where the positron beam load is placed.

In this approach, an appropriately spaced drive–witness electron beam configuration described earlier is focused onto a thin conversion target located right inside the plasma [44]. The electron beam generates an electromagnetic shower, consisting mainly of secondary electrons, positrons and photons. If the wire is thin enough, the emittance of the primary electron beam is not seriously degraded and the drive–witness structure is preserved. Furthermore, the shower creates an identical, albeit a low-current positron bunch structure that can be used to probe the wake. Figure 11(a) shows the drive electron and the witness positron bunches obtained with this method, as well as the longitudinal component of the wakefield (E_z) driven in a plasma with a density of $5 \times 10^{16}\,\mathrm{cm}^{-3}$. The drive electron bunch can still drive a nonlinear plasma wake containing a blowout region. Such a plasma wake includes a region where the wake fields are both focusing and accelerating for positrons overlapping the witness bunch (figure 11(a) and (b)). The witness positron bunch can gain up to 6 GeV in 1 m of plasma, and be accelerated with a relatively narrow energy spread (figure 11(c)).

Accelerating a high-charge positron bunch on the wake driven by an electron bunch requires accelerating and compressing individual bunches in the SLAC linac. This is possible because beams can be extracted from the electron and positron damping rings on the same

linac pulse [45]. The electrons and positrons will have to be separated by a 1/2 rf wavelength (5 cm) in the SLAC linac to accelerate both to high energies. This is accomplished by modifying the magnetic compression chicane in FACET Sector 20 to simultaneously accommodate both electron and positron beams. The initial path length difference of 5 cm can be reduced to the appropriate $\sim$100 μm by using a double chicane [46]. Separate control of the electron and positron beam parameters (charge, length and spacing) will allow for the systematic study of accelerated positron beam characteristics.

4. Conclusion

In this paper we have described the second generation of PWFA experiments at the FACET facility that is currently under construction at SLAC. The main goal of these experiments is to demonstrate the significant energy gain of electron and positron bunches in a single high-gradient PWFA stage. To be useful for future collider applications, the acceleration process must preserve the incoming beam emittance, accelerate a sufficient charge with a small energy spread and have a high drive to witness bunch energy transfer efficiency. Initial studies and simulation indicate that these goals can be achieved with the electron beam parameters afforded by FACET. Further optimization of positron acceleration by wakefields will be performed after the initial series of experiments described here. As the only facility in the world to have high-energy, high-current electron and positron beams, the FACET facility will advance the frontier of plasma accelerators, allow exploration of new phenomena and no doubt yield unexpected results.

Acknowledgments

This work was supported by US DOE grants DE-FG02-92ER40727 and DE-FC02-07ER41500 (UCLA), DE-FG03-92ER40745 (USC), DE-AC02-76SF00515 (SLAC) and NSF grants PHY-0936266 and PHY-0904039 (UCLA) and ECS-9632735 (USC). We thank all our collaborators on the E157, 162, 164 and 167 experiments carried out at SLAC as well as the OSIRIS and QuickPIC team members at IST in Portugal.

References

[1] Joshi C and Katsouleas T 2003 *Phys. Today* **47**
[2] Muggli P and Hogan M J 2009 *C. R. Phys.* **10** 116
[3] Joshi C 2007 *Phys. Plasmas* **14** 05501
[4] Muggli P *et al* 2001 *Nature* **411** 43
Muggli P *et al* 2001 *Phys. Rev. ST Accel. Beams* **4** 091391
[5] Wang S *et al* 2002 *Phys. Rev. Lett.* **88** 135004
Johnson D *et al* 2006 *Phys. Rev. Lett.* **97** 175003
[6] Oz E *et al* 2007 *Phys. Rev. Lett.* **98** 084801
Kirby N *et al* 2009 *Phys. Rev. ST Accel. Beams* **12** 051302
[7] O'Connell C L *et al* 2006 *Phys. Rev. ST Accel. Beams* **9** 101301
[8] Blumenfeld I *et al* 2007 *Nature* **445** 741
[9] Seryi A *et al* 2009 *Proc. Particle Accelerator Conf.* (*Vancouver, BC, May 4–8, 2009*)

[10] Rosenzweig J B *et al* 1988 *Phys. Rev. Lett.* **61** 98
Barov N *et al* 1998 *Phys. Rev. Lett.* **80** 81
[11] Hogan M *et al* 2000 *Phys. Plasma* **7** 2241
[12] http://www.ee.ucla.edu/~plasma/FACET_links.html
[13] Chen P *et al* 1995 *Phys. Rev. Lett.* **54** 693
[14] Muggli P *et al* 1999 *IEEE Trans. Plasma Sci.* **27** 791
[15] Rosenzweig J *et al* 1991 *Phys. Rev.* A **44** R6189
[16] Joshi C *et al* 2002 *Phys. Plasmas* **9** 1845
[17] Lu W *et al* 2005 *Phys. Plasmas* **12** 63101
[18] Lu W *et al* 2006 *Phys. Rev. Lett.* **96** 165002
[19] Lu W *et al* 2006 *Phys. Plasmas* **13** 56709
[20] Rosenzweig J B 1987 *Phys. Rev. Lett.* **58** 555
[21] See paper by Lu W *et al* 2010 *New J. Phys.* at press
[22] Muggli P *et al* 2004 *Phys. Rev. Lett.* **93** 014802
Hogan M *et al* 2005 *Phys. Rev. Lett.* **95** 054802
Muggli P *et al* 2010 *New J. Phys.* **12** 045022
[23] Clayton C E *et al* 2002 *Phys. Rev. Lett.* **88** 154801
[24] Hemker R *et al* 2000 *Phys. Rev. ST Accel. Beams* **3** 061301
[25] Huang C *et al* 2006 *J. Comput. Phys.* **217** 658
[26] Krejcik P *et al* 2003 Commissioning of the SPPS linac bunch compressor, *Proc. Particle Accelerator Conf. (Portland, Oregon May 12–16, 2003)* (Piscataway, NJ: IEEE) pp 423–5
[27] Vidal C R and Cooper J 1969 *J. Appl. Phys.* **40** 3370
[28] Zhou M 2008 *PhD Thesis* UCLA
[29] Muggli P *et al* 2008 *Phys. Rev. Lett.* **101** 054801
[30] Borland M 2000 *Advanced Photon Source* LS-287
[31] Nelson W R *et al* 1985 SLAC-R-265
[32] Borland M *et al* 2003 *Proc. PAC 03 Conf.* p 3461
[33] Bane K L F, Chen P and Wilson P B 1985 *IEEE Trans. Nucl. Sci.* **NS-32** 3524
[34] Rosenzweig J *et al* 2005 *Phys. Rev. Lett.* **95** 195002
[35] Gholizadeh R *et al* 2007 *Proc. PAC 07 Conf.* p 3067
[36] Gholizadeh R *et al* 2009 *Phys. Rev. Lett.* submitted
[37] Blue B *et al* 2003 *Phys. Rev. Lett.* **90** 214801
[38] Hogan M *et al* 2003 *Phys. Rev. Lett.* **90** 205002
[39] Muggli P *et al* 2008 *Phys. Rev. Lett.* **101** 055001
[40] Lee S *et al* 2002 *Phys. Rev. ST Accel. Beams* **5** 011001
[41] Yakimenko V and Ischebeck R 2006 Advanced accelerator concepts *AIP Conf. Proc.* **877** 158
[42] Ng J S T *et al* 2001 *Phys. Rev. Lett.* **87** 244801
[43] Huang C *et al* 2007 *Phys. Rev. Lett.* **99** 255001
[44] Wang X *et al* 2008 *Phys. Rev. Lett.* **101** 124801
[45] Adolphsen C *et al* 2003 *Proc. PAC 99 Conf.* p 3477
[46] Hogan M J and Seryi A private communication